Histol Histopathol (2020) 35: 111-124

http://www.hh.um.es

Histology and Histopathology
From Cell Biology to Tissue Engineering

Bone biology in postnatal Wistar rats following hypoxia-reoxygenation

Rita Hameister[1], Christoph H. Lohmann[2], S. Thameem Dheen[1], Gurpal Singh[3] and Charanjit Kaur[1]

[1]Department of Anatomy, Yong Loo Lin School of Medicine, National University of Singapore, Singapore, [2]Otto-von-Guericke University, Department of Orthopaedic Surgery, Magdeburg, Germany and [3]University Orthopaedics, Hand and Reconstructive Microsurgery Cluster, National University Health System, Singapore

Summary. Hypoxia response pathways have a central role in normal and abnormal bone biology but the effect of systemic hypoxia-reoxygenation on bone is not clear. Following hypoxic exposure, aberrant synthesis, folding and trafficking of proteins has been reported to occur, which can result in endoplasmic reticulum (ER) stress and may finally cause cell death. This study aimed to examine the effect of systemic hypoxia-reoxygenation injury on bone biology in postnatal rats. Immunoexpression of HIF-1α and VEGF was upregulated in femurs of newborn Wistar rats in response to systemic hypoxia-reoxygenation. Along with that, increased apoptosis of osteoblast precursors, osteoblasts, osteocytes and endothelial cells was observed in comparison to femurs of control animals by transmission electron microscopy, TUNEL staining and immunoexpression of cleaved caspase-3. The viability of osteoclasts was not affected. After hypoxia-reoxygenation, ER stress was observed in the osteoblasts and osteocytes as indicated by dilatation of the ER and enhanced immunoexpression of the ER stress marker GRP78. Localisation of collagen α1 immunoreaction was widespread in the bone matrix of control femurs but was confined to the osteoblasts and osteocytes in response to hypoxia-reoxygenation. In support of these findings, *in vitro* work showed reduced viability of osteoblast-like SaOs-2 cells and upregulation of GRP78 protein expression in them by western blotting following exposure to hypoxia. This suggests that systemic hypoxia-reoxygenation may disturb bone biology in postnatal Wistar rats by inducing ER stress and apoptosis in osteoblasts and osteocytes, without affecting the viability of osteoclasts. More in-depth research is needed to confirm causality between ER stress and apoptosis of osteoblasts and osteocytes.

Key words: Apoptosis, Bone biology, Endoplasmic reticulum stress, Hypoxia, Osteoblast

Offprint requests to: Charanjit Kaur, PhD, MBBS, BSc, Professor, Department of Anatomy, Yong Loo Lin School of Medicine, National University of Singapore, Blk MD10, 4 Medical Drive, 117594 Singapore, Singapore. e-mail: antkaurc@nus.edu.sg

DOI: 10.14670/HH-18-143

Introduction

Bone homeostasis is characterized by a balance between bone formation and bone resorption. It is primarily regulated by osteoblasts, osteocytes and osteoclasts in close relationship with endothelial cells of invading blood vessels (Parfitt, 1994). Hypoxia response pathways have been suggested to play a fundamental role in normal bone biology such as skeletal development (Araldi and Schipani, 2010) as well as abnormal bone biology. Examples of the presence of a hypoxic microenvironment in bone diseases include osteoarthritis, bone metastasis, osteoporosis, non-traumatic osteonecrosis, and metal wear-induced failure of joint replacements (Maes et al., 2012; Seamon et al., 2012; Miyauchi et al., 2013; Samelko et al., 2013). In addition to localized hypoxia, systemic hypoxia may occur for various reasons such as cardiac arrest, lung dysfunction and anaemia (Austen et al., 1963; Andersen, 2001; Kent et al., 2011). Hypoxia is an underlying factor

reported in complications occurring because of preterm birth (Reynolds, 1977).

Hypoxia induces the expression of hypoxia-inducible factors (HIFs), heterodimeric transcription factors that are essential in regulating oxygen homeostasis (Majmundar et al., 2011). HIFs also control several pathways in relation to metabolism, angiogenesis, cell differentiation and apoptosis in both normal and pathologic conditions (Nizet and Johnson, 2009). Along with that, HIFs have emerged as essential regulators in endochondral bone development (Araldi and Schipani, 2010). Among others, HIF-1α increases transcriptional activation of many genes, including vascular endothelial growth factor (VEGF). VEGF has angiogenic potential and has further been described to act as a proinflammatory cytokine (Reinders et al., 2003), to promote vascular permeability (Liu et al., 1995; Kaur et al., 2009) and to cause vasodilatation of the blood vessels (Rathnasamy et al., 2015). In addition to that, VEGF can affect bone biology by stimulating bone resorption through enhanced differentiation, survival and chemotaxis of osteoclasts (Niida et al., 1999; Nakagawa et al., 2000; Henriksen et al., 2003).

Following hypoxia, the function of oxygen-consuming cell organelles such as the endoplasmic reticulum (ER) can become compromised (Schönenberger and Kovacs, 2015). Alterations in redox state, cellular energy level and Ca^{2+} homeostasis can cause aberrant protein synthesis and folding, leading to the accumulation of misfolded proteins within the ER. This condition is known as ER stress and may ultimately result in cell death (Tabas and Ron, 2011). A wide range of bone-related diseases including experimental periodontitis (Yamada et al., 2015), unloading-induced disuse osteoporosis (Li et al., 2017) and osteogenesis imperfecta (Lisse et al., 2008) emphasize a link between ER stress and disturbed bone homeostasis.

Based on the above, this study aimed to examine the effect of hypoxia-reoxygenation on bone biology. The primary objective was to assess the effect of systemic hypoxia-reoxygenation on the viability of cells involved in maintenance of bone homeostasis. The secondary objective was to assess osteoblasts/osteocytes for hypoxia-induced signs of ER stress that may affect bone formation.

Material and methods

Animal model

To study the effect of hypoxia-reoxygenation on femurs, one-day-old wild type male and female Wistar rats (n=54) were used in this study. Twenty-seven rats were subjected to systemic hypoxia using a multigas chamber (Sanyo Biomedical Electrical; model MCO-18M) filled with 5% O_2 and 95% N_2 for 2 hours. The animals were allowed to recover under normoxic conditions in room air for 1, 3 or 7 days (n=9 at each time point) before sacrificing. Twenty-seven age-matched rats were used as controls. The experiments were approved by the Institutional Animal Care and Use Committee, National University of Singapore. The animals were housed under standard conditions with unrestricted cage activity and were provided with food and water ad libitum.

Sample preparation

After induction of anaesthesia with medetomidine-ketamine, rats were perfused transcardiacally with 2% periodate-lysine-paraformaldehyde for histochemichal stainings, 2% paraformaldehyde (PF) + 3% glutaraldehyde for electron microscopic and 4% PF for all other light microscopic studies. Whole femurs were dissected, soft tissue was removed and bones were immersed in the respective fixative for 24 hours at 4°C. Next day, the samples were washed with tap water. All samples were decalcified by immersion in 10% diamine tetraacetic acid at 4°C (Liu et al., 2017).

Transmission electron microscopic studies

Ultrastructural changes in the femurs of control and hypoxia-reoxygenation injury animals were analysed by transmission electron microscopy. Femurs were postfixed with 1% osmium tetroxide for 2 hours and were dehydrated in a series of ascending ethanol concentrations and gradually infiltrated with increasing concentrations of araldite mixture. Samples were allowed to polymerize for 24 hours. Ultrathin cross-sections of 100 nm thickness were cut with an ultramicrotome, picked up on copper grids and stained with lead citrate and were viewed under the Joel JEM 1220 transmission electron microscope.

Light microscopic studies

Decalcified femurs were embedded in paraffin following routine protocol. Femurs were sectioned longitudinally at 4 μm thickness. Sections were deparaffinised in xylene and rehydrated through a series of descending concentration of alcohol.

Haematoxylin-Eosin staining

Slides were immersed in filtered Shandon Haematoxylin for 10 min at room temperature, rinsed in distilled water and differentiated in differentiation fluid for 30 sec followed by washing in tap water for 10 min until the nuclei were blue in colour. Subsequently, slides were washed in distilled water and stained with alcoholic eosin for 1 min and dehydrated in a series of ascending concentration of alcohol, cleared with Clearane. Sections of femurs were mounted using Permount medium (Fisher Scientific, USA).

Immunohistochemistry

Antigen retrieval was performed in 0.1M citrate buffer (pH=6) overnight at 60°C. Endogenous peroxidise activity was blocked with 3% hydrogen peroxide in methanol for 20 min at room temperature. Subsequently, the sections were washed with phosphate buffered saline (PBS) followed by the incubation with monoclonal primary antibodies diluted in PBS in a humid chamber overnight at room temperature: HIF-1α (1:50, sc-10790, Santa Cruz Biotechnology) and vascular endothelial growth factor (VEGF) (1:75, sc-7269, Santa Cruz Biotechnology) for the hypoxia-signalling response, cleaved caspase-3 (1:100, #9661, Cell Signaling Technology) for apoptosis, GRP78 (1:25, sc-376768, Santa Cruz Biotechnology, Inc., USA) and collagen α1 (1:50, sc-293182, Santa Cruz Biotechnology) for the ER stress response. Next day, after washing in PBS, sections were incubated with a biotin-conjugated secondary antibody (anti-mouse IgG, 1:200 each) at room temperature for 60 min and subsequently washed with PBS. The sections were incubated in Avidin Biotin Complex (Vector Laboratories) for 60 minutes at room temperature, washed with PBS and then soaked in Tris-buffered saline. The peroxidise activity was demonstrated by 3,3-diaminobenzidine (Sigma-Aldrich,). All sections were counterstained with Haematoxylin, dehydrated in alcohol, cleared with Clearane and mounted using Permount medium (Fisher Scientific).

TUNEL staining

To determine apoptotic cell death in femurs of control and hypoxia-reoxygenation animals, terminal deoxynucleotidyl transferase dUTP nick end labelling (TUNEL) staining, a method to detect DNA fragmentation by labelling the 3' hydroxyl termini in the double-strand DNA breaks generated during apoptosis, was performed using the *In Situ* Apoptosis Death Detection Kit (abcam, ab206386) according to the manufacturer's instructions. This kit is based on diaminobenzidine reaction. Methyl green was used for counterstaining.

Evaluation of immunohistochemical markers

A BX51 microscope (Olympus Corporation) equipped with a DP50 Microscope Digital Camera System (Olympus Corporation) was used to acquire all light microscopic images. Immunohistochemical markers were evaluated using "ImageJ", an image-processing program developed at the National Institute of Health, by manually counting stained and unstained osteoblasts and osteocytes, respectively, with the help of the "grid" and "cell counter" plugins. Three slides from each femur were analyzed using the x40 objective. Cells that were located subperiosteally were considered as pre-osteoblasts and were not included in the analysis. The metaphyseal-diaphyseal junction was chosen as the region of interest as this is where active bone development is taking place in the newborn. This area showed consistently prominent staining.

Cell culture

Human SaOs-2 cells (ACC-243, DSMZ) were cultured in 85% McCoy's 5A culture medium (gibco), supplemented with 15% heat-inactivated fetal calf serum (HyClone) and 1% penicillin/streptomycin (HyClone) at 37°C and in 5% CO_2 in a humified atmosphere. The SaOs-2 cell line is well characterized and shares properties with primary human osteoblasts, resembling mature osteoblasts (Pautke et al., 2004). The osteoblast-like cells were subjected to hypoxia by placing them for 4 hours in a multigas chamber (Sanyo Biomedical Electrical; model MCO-18M) containing 92%N_2, 5%CO_2 and 3%O_2 at 37°C. The control cultures were incubated at 95% O_2 and 5% CO_2 at 37°C.

Trypan blue exclusion test

The viability of osteoblast-like cells after hypoxic exposure was examined by Trypan blue exclusion test. Cells that took up Trypan blue (Sigma-Aldrich) were considered as non-viable as the dye can transverse the cell membrane of dead cells. Cells that remained unstained were considered as viable.

Immunofluorescence

Immunofluorescence was carried out to examine the expression of cleaved caspase-3 in osteoblast-like cells following hypoxia as compared to control cells. In brief, cultured cells were fixed in 4% PF and blocked with 3% bovine serum albumin (BSA) for 1 hour. The cells were then incubated with the primary anti-cleaved caspase-3 antibody (1:200, #9661, Cell Signaling Technology) overnight at 4°C, followed by incubation with the secondary FITC-conjugated antibody (Sigma-Aldrich). Subsequently, the sections were mounted with a fluorescence mounting medium containing DAPI (DAKO) after being washed. Immunoexpression of cleaved caspase-3 was assessed by confocal microscopy (Olympus, FV 1000 Olympus Optical Co. Ltd.). Bleedthrough was avoided by use of sequential scanning mode.

Western blotting

To examine change in protein expression of the ER stress marker GRP78 in osteoblast-like cells following hypoxia, western blotting was performed. Protein was extracted from SaOs-2 cells with a protein extraction reagent containing protease inhibitors (Thermo Scientific). Protein concentration was determined by the Bradford method using BSA (Sigma-Aldrich) as a standard (Bradford, 1976). Samples of supernatant

containing 20 μg protein were heated to 95°C for 5 min and were separated by sodium dodecyl sulphate-poly-acrylamide gel electrophoresis gels in a Mini-Protean 2 apparatus (Bio-Rad). Protein bands were electroblotted onto polyvinylidene difluoride membranes (Bio-Rad) and blocked with 5% (w/v) nonfat dried milk. Subsequently, the membranes were probed with GRP78 antibody (1:500, #3177, Cell Signaling Technology) overnight at 4°C, followed by incubation with the secondary antibody conjugated with horseradish peroxidise (Thermo Scientific). For loading control, the membranes were incubated with anti-ß-actin antibody (1:5,000, sc-47778, Santa-Cruz Biotechnology). Specific binding was revealed by using an enhanced chemiluminescence kit (Thermo Scientific). Precision prestained standard (Thermo Scientific) were used as molecular weight markers. The immunoreactive bands captured on the X-ray films were quantified using a densitometer (GS-800 Calibrated Densitometer, Bio-Rad) and Quantity One software (Bio-Rad). The experiments were performed as biological triplicates.

Statistical analysis

In the animal model, the percentage of positively stained osteoblasts and osteocytes for the various immunohistochemical markers is presented as median and range. To compare the expression of immunohistochemical markers in hypoxic and control rats, a Mann-Whitney-U test was performed. For *in vitro* studies, a student's t-test was performed and data are presented as mean ± standard deviation. A p-value <0.05 was considered to be statistically significant and represented as #p<0.05 for animal work and as *p<0.05 and ***p<0.001 for *in vitro* experiments.

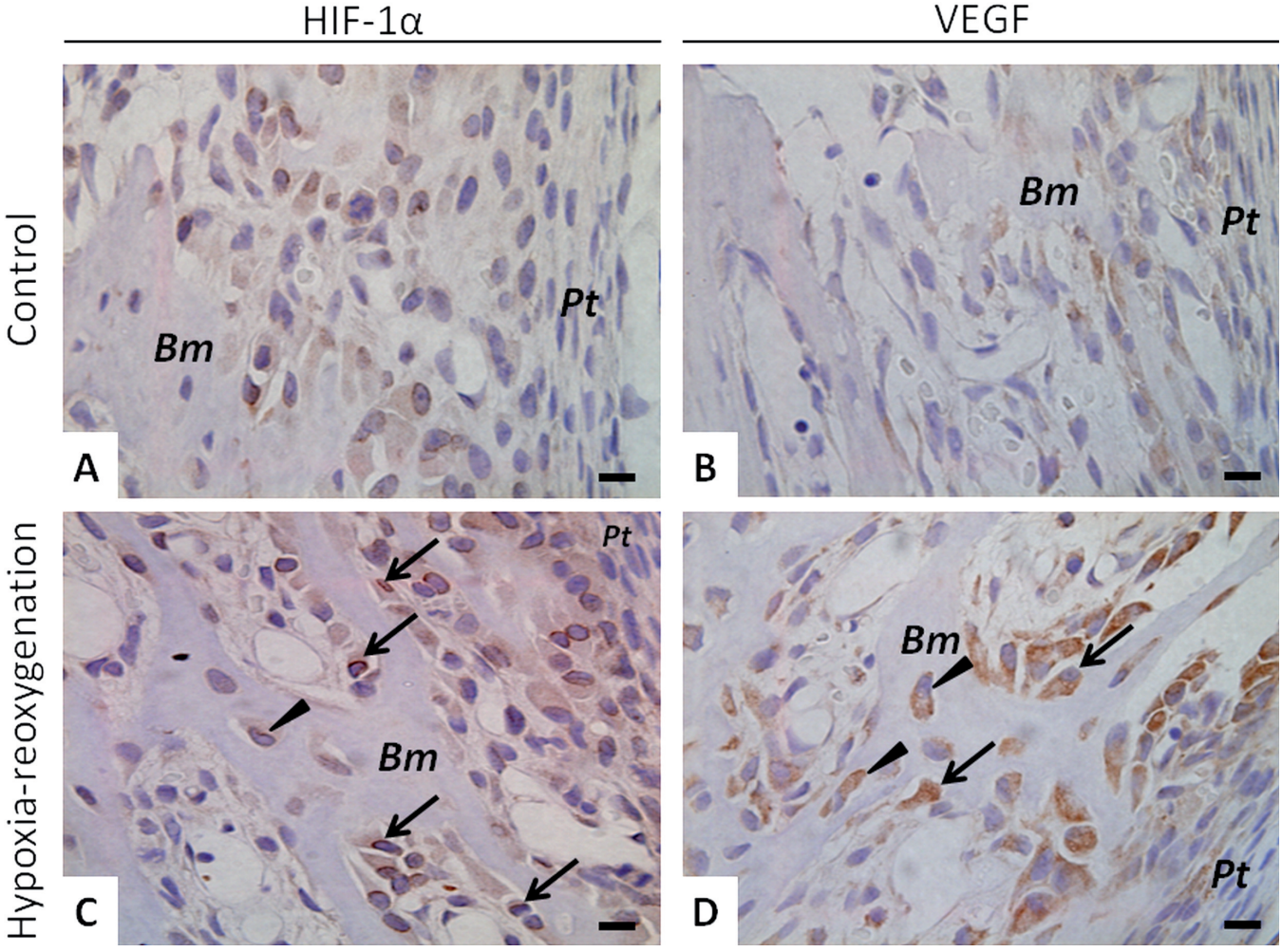

Fig. 1. Light microscopic images of femurs obtained from Wistar rats at 3 days after hypoxia-reoxygenation injury **(C, D)** and age-matched controls **(A, B)** displaying immunoexpression of hypoxia-inducible factor-1α (HIF-1α) **(A, C)** and vascular endothelial growth factor (VEGF) **(B, D)** in osteoblasts (arrows) and osteocytes (arrowheads). Bm: bone matrix, Pt: periosteum. Scale bars: 10 μm.

Results

Upregulation of hypoxia-inducible factor-1α and vascular endothelial growth factor in response to systemic hypoxia-reoxygenation injury

HIF-1α protein and its downstream target VEGF were detected by immunohistochemistry in osteoblasts, newly embedded osteocytes, osteoblast precursors in the inner layer of the periosteum, osteoclasts and in some bone marrow cells in all femurs. Its expression was increased in response to systemic hypoxia-reoxygenation (Fig. 1, Table 1). The increase in the proportion of HIF-1α and VEGF-expressing cells was noted to be statistically significant for osteoblasts at day 3 and day 3+7 after exposure to hypoxia, respectively. For osteocytes, the increase in the proportion of cells expressing HIF-1α and VEGF was statistically significant at day 3+7 and day 3 after exposure to hypoxia, respectively. In both groups, control and hypoxia-reoxygenation, a gradient in the immunoexpression of HIF-1α and VEGF was noted that was higher towards the endosteal surface of the femur as compared to the centre of the bone marrow cavity. A trend towards a higher immunoexpression of HIF-1α and VEGF was also observed towards the metaphyseal/diaphyseal junctions of the femur as compared to the middle of the diaphysis.

The effects of systemic hypoxia-reoxygenation injury on cell viability

Following hypoxia-reoxygenation, empty-looking and large lacunae were recognized in the bone trabeculae. Along with that, an upregulation of cleaved caspase-3 expression was observed in osteoblast precursors, osteoblasts and osteocytes, indicating that these cells were apoptotic (Table 1). The increase in the

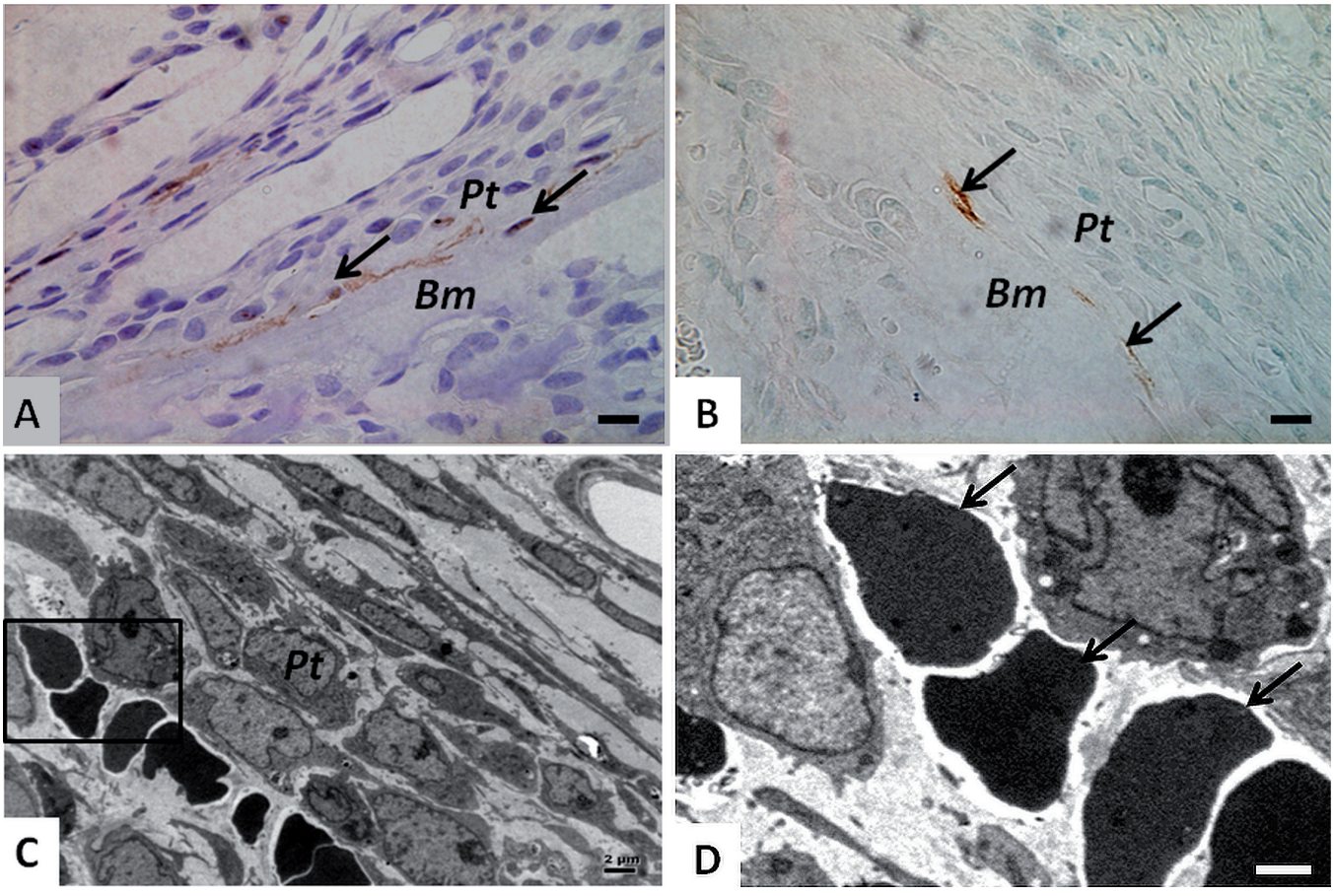

Fig. 2. Light and electron microscopic images displaying death of osteoblast precursors in the inner layer of the periosteum in femurs obtained from Wistar rats at 3 days after hypoxia-reoxygenation injury. **A** displays osteoblast precursors (arrows) showing immunoexpression for cleaved caspase-3. **B** displays osteoblast precursors (arrows) with terminal deoxynucleotidyl transferase dUTP nick end labelling staining. At the electron microscopic level, degeneration of osteoblast precursors (arrows) is evidenced by extensive darkening **(C, D).** The squared area in **C** is displayed at higher magnification in **D**. Bm: bone matrix, Pt: periosteum. Scale bars: A, B, 10 μm; C, 2 μm; D, 1 μm.

Table 1. Percentage of positively stained osteoblasts and osteocytes in postnatal Wistar rats at 1, 3 and 7 days after hypoxic exposure and their corresponding controls using the immunohistochemical marker hypoxia-inducible factor-1α (HIF-1α), vascular endothelial growth factor (VEGF), cleaved caspase-3 and glucose-related protein78 (GRP78).

Marker	Time	% positive osteoblasts [median (range)]			% positive osteocytes [median (range)]		
		Control	Hypoxia	p-value	Control	Hypoxia	p-value
HIF-1α	1 day post intervention	0.5 (0-17)	2 (0-18)	0.394	2 (0-11)	10.5 (4-22)	0.074
	3 days post intervention	8 (2-23)	30.5 (12-45)	0.011#	12 (2-15)	37.5 (15-44)	0.015#
	7 days post intervention	4.5 (1-9)	21 (4-55)	0.058	4 (0-10)	17 (9-43)	0.004#
VEGF	1 day post intervention	0.5 (0-3)	2 (0-7)	0.253	0	0	>0.999
	3 days post intervention	10.5 (4-23)	29 (12-49)	0.046#	8.5 (0-25)	30 (7-41)	0.026#
	7 days post intervention	0.5 (0-7)	9.5 (2-12)	0.017#	0 (0-0)	0.5 (0-1)	0.182
Cleaved Caspase-3	1 day post intervention	0	1.5 (1-4)	0.002#	7 (0-24)	32.5 (7-50)	0.024#
	3 days post intervention	0 (0-0.5)	1 (0-2)	0.015#	0 (0-8)	21.5 (3-29)	0.004#
	7 days post intervention	0 (0-1)	2 (0-5)	0.033#	4 (0-12)	25 (19-46)	0.002#
GRP78	1 day post intervention	13 (8-26)	14.5 (10-21)	0.721	0 (0-14)	15 (7-45)	0.013#
	3 days post intervention	8 (4-26)	22.5 (19-30)	0.020#	4 (0-7)	14 (4-20)	0.013#
	7 days post intervention	13.5 (10-21)	26 (14-50)	0.041#	7 (0-17)	23 (17-38)	0.007#

Significant differences in immunoexpression between hypoxic and control femurs are expressed as #p<0.05.

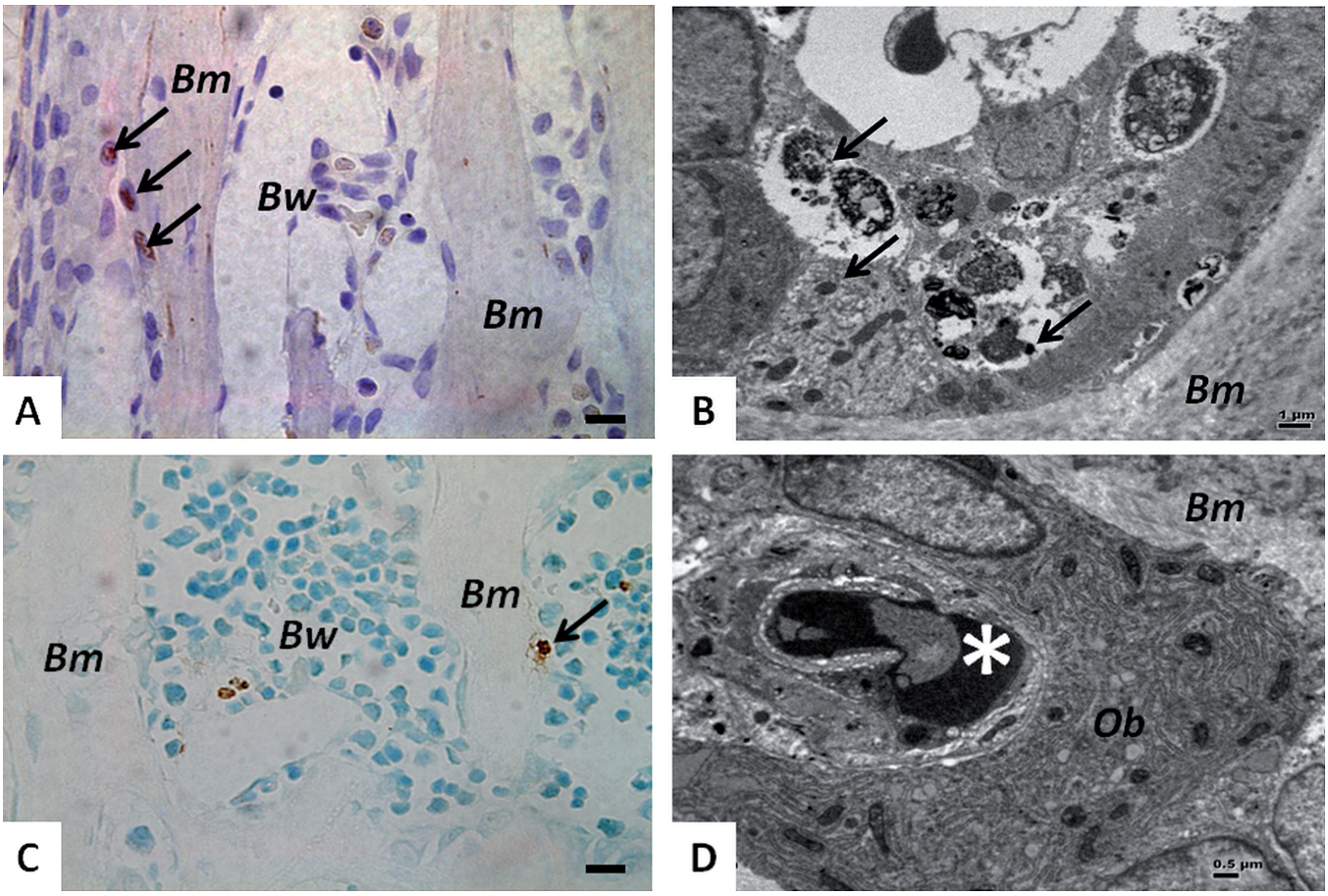

Fig. 3. Light and electron microscopic images displaying degeneration of osteoblasts in femurs obtained from Wistar rats at 3 days after hypoxia-reoxygenation injury. **A** shows immunoexpression of cleaved caspase-3 in osteoblasts (arrows). **C** shows terminal deoxynucleotidyl transferase dUTP nick end labelling staining of an osteoblast (arrow). Osteoblasts undergoing necrosis (arrows) are displayed in **B**. An apoptotic osteoblast (asterisk), indicated by the condensation of the chromatin, is seen in close association with a viable osteoblast (Ob) in **D**. Bm: bone matrix, Bw: bone marrow, Ob: osteoblast. Scale bars: A, 10 μm; B, 1 μm; C, 10 μm; D, 0.5 μm.

proportion of osteoblasts and osteocytes expressing cleaved caspase-3 after exposure to hypoxia was statistically significant at all three points of time. These results were strengthened by TUNEL staining and were further supported by transmission electron microscopy, where apoptotic and necrotic cells were detected (Fig. 2-4). *In vitro*, significantly reduced viability and enhanced immunoexpression for cleaved caspase-3 following hypoxic injury was noted in osteoblast-like SaOs-2 cells (Fig. 5). In addition to the cells of the osteogenic lineage, the endothelial cells in the animal model showed necrotic changes, which were evident by large vacuoles (Fig. 6). Apoptotic cells were also seen in close association with the endothelial cells. Hypoxia-reoxygenation did not appear to affect the viability of osteoclasts as assessed by light and transmission electron microscopy (Data not shown).

Systemic hypoxia-reoxygenation injury induces endoplasmic reticulum stress in osteoblasts and osteocytes

In the animal model, extensive dilation of the rough ER in hypoxia-reoxygenation injury osteoblasts and osteocytes as compared to control osteoblasts and osteocytes (Fig. 7) was revealed by transmission electron microscopy. This was accompanied by a strong positive immunoreaction for the ER stress marker GRP78 (Fig. 8A,B, Table 1). The increase in the proportion of GRP78-expressing cells was statistically significant for osteoblasts at day 3+7 after exposure to hypoxia and for osteocytes at all three points of time.

The findings derived from animal work were supported by a significant upregulation of GRP78 protein in cultured human osteoblast-like cells (Fig. 9).

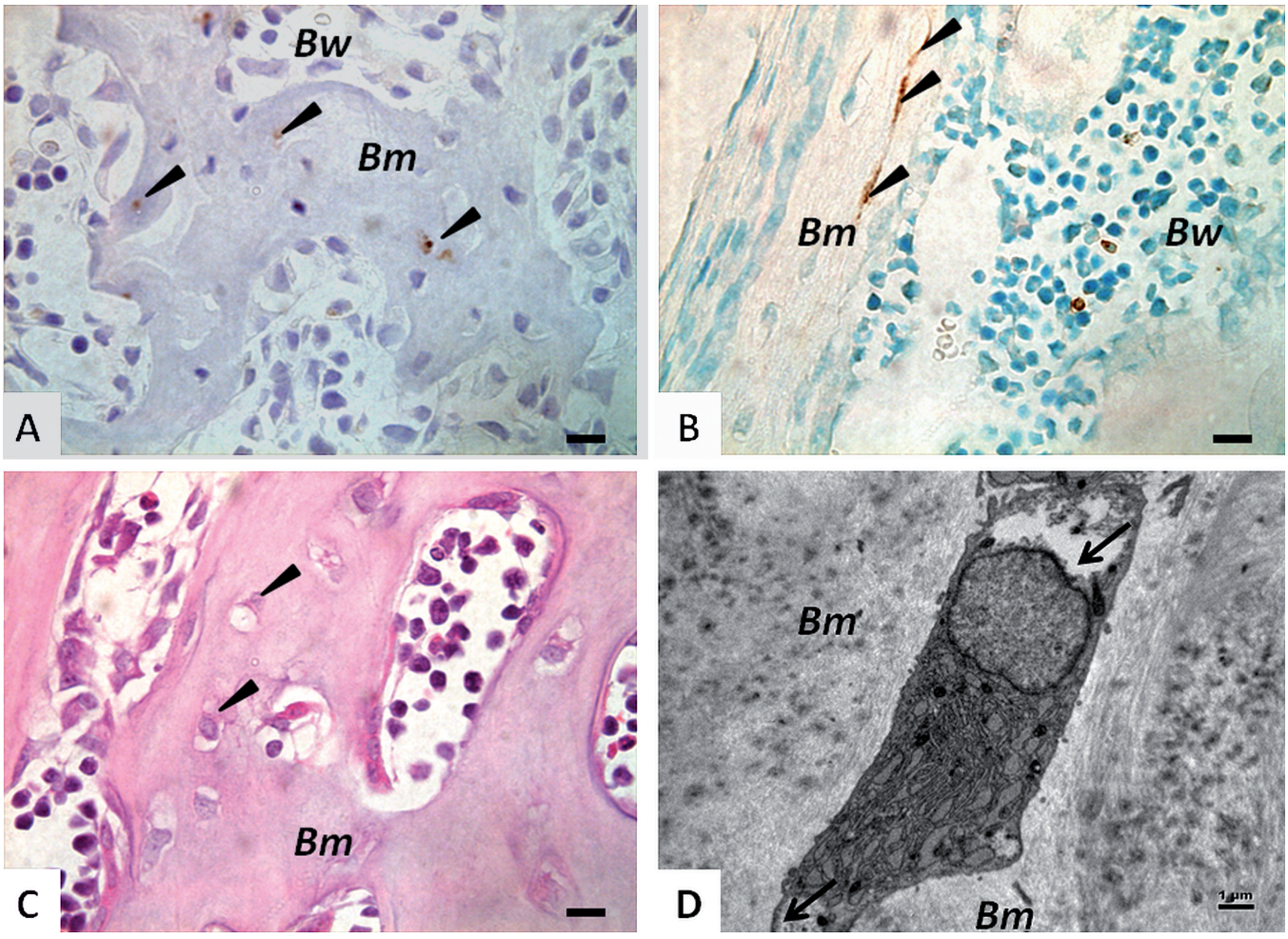

Fig. 4. Light and electron microscopic images displaying degeneration of osteocytes in femurs obtained from Wistar rats at 3 days after hypoxia-reoxygenation injury. **A** shows immunoexpression of cleaved caspase-3 in osteocytes (arrowheads). **B** shows terminal deoxynucleotidyl transferase dUTP nick end labelling staining of osteocytes (arrowheads). Degeneration of osteocytes is reflected by large and empty-looking lacunae (arrowheads) in Haematoxylin-Eosin stained slides **(C)**. At the electron microscopic level, degeneration of osteocytes (arrows) is evidenced by the presence of large vacuoles in the cytoplasm **(D)**. Bm: bone matrix, Bw: bone marrow. Scale bars: A-C, 10 μm; D, 1 μm.

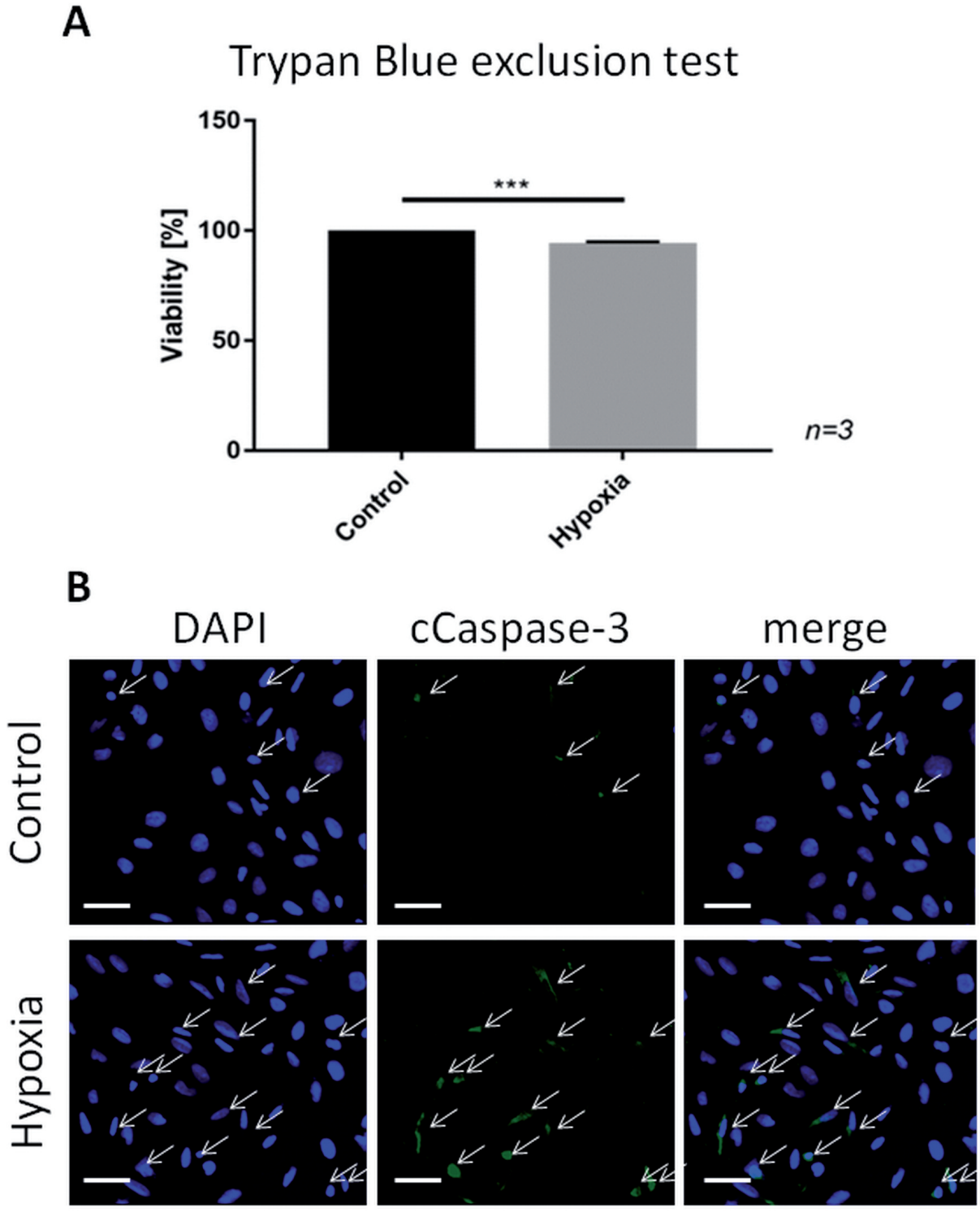

Fig. 5. A shows a bar graph of the viability of normal and hypoxic osteoblast-like SaOs-2 cells as examined by Trypan blue exclusion test. The significant change in viability between hypoxic and control cells is expressed as ***p<0.001. **B** shows confocal images displaying the expression of cleaved caspase-3 in normal and hypoxic osteoblast-like SaOs-2 cells. Nuclei are stained with DAPI. Scale bars: 50 μm.

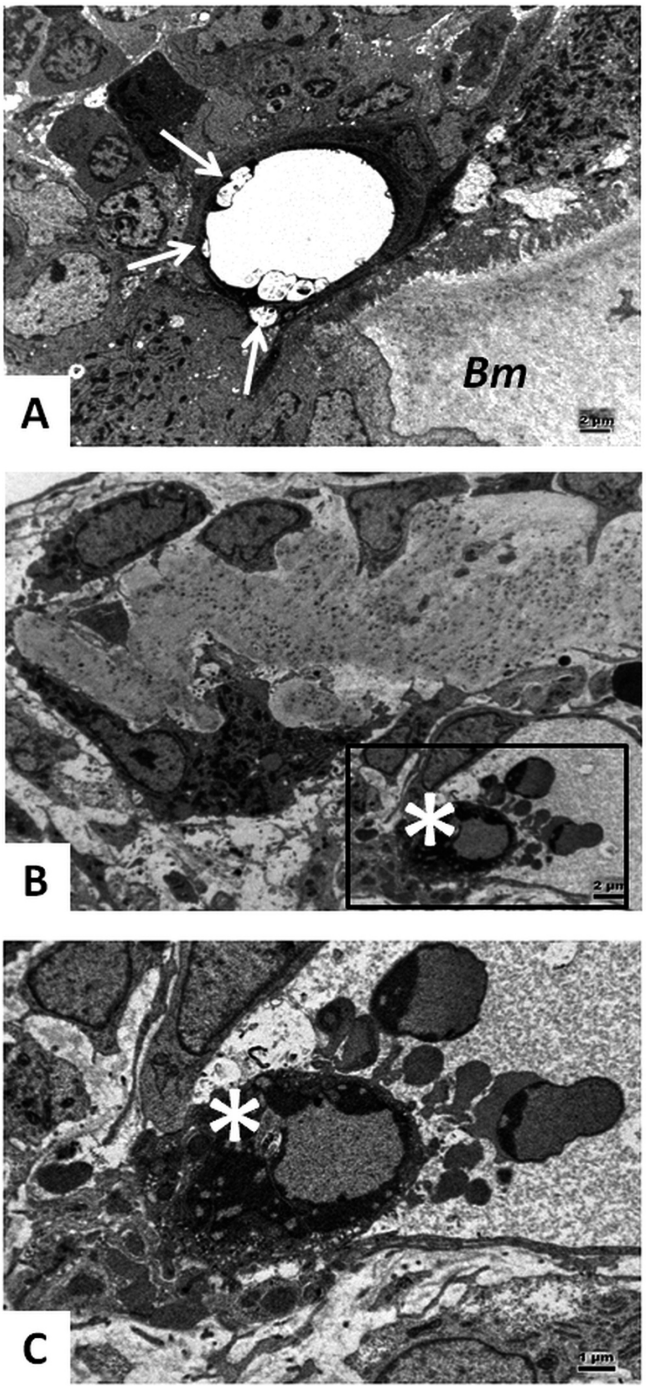

Fig. 6. Electron microscopic images displaying degeneration of the endothelial cells in small blood vessels within the bone marrow cavity of femurs obtained from Wistar rats at 3 days after hypoxia-reoxygenation injury. Degeneration is evidenced by extensive vacuolation (arrows) of the endothelial cell in a capillary in **A**. An apoptotic cell (asterisk), indicated by the condensation of the chromatin and blebbing of the cell surface along with the release of apoptotic bodies, was noted in close association with the endothelial cells of a sinusoid **(B, C)**. The squared area in **B** is displayed at higher magnification in **C**. Bm: bone matrix. Scale bars: A, B, 2 μm; C, 1 μm.

In the animal model, collagen α1 immunoreaction was widespread in control femurs within the bone matrix in the trabeculae but was confined to osteoblasts and osteocytes in response to hypoxia-reoxygenation (Fig. 8C,D).

Discussion

The results from our animal work suggest that systemic hypoxia-reoxygenation may disturb bone biology in postnatal Wistar rats. Studies reporting cellular responses towards hypoxia have been mainly performed using cell lines (Lennon et al., 2001; Potier et al., 2007; Huang et al., 2012; Xu et al., 2015; Montesi et al., 2016; RajendranNair et al., 2017). While *in vitro* studies may be particularly useful in enhancing a mechanistic understanding of the effect of hypoxia on cells, a number of limitations are to be noted. Most importantly, cells removed from their natural environment lack the extensive interactions among other cells and tissues. In addition to that, cell maintenance in artificial conditions may not be reflective of the actual microenvironment and may, therefore, alter cellular behaviour (Hartung and Daston, 2009).

Previous animal studies investigating the effect of hypoxia on bone were based on ischemia-reperfusion injury and included clamping of the femoral artery and/or application of a tourniquet (Hsieh et al., 2001; Zhang et al., 2017). We used a multigas chamber to study the effects of systemic hypoxia-reoxygenation on bone to exclude that the observed effects in our experimental model may be secondary to surgical effects. The present experimental model of hypoxic injury has been extensively used to investigate the effects of low oxygen tension on the developing brain without causing important adverse events (Rathnasamy et al., 2011; Kaur et al, 2014). Thus, we believe that it is suitable to induce hypoxia-reoxygenation injury. Because others reported that an ischemia time of 2-4 hours induces injury of the cortical bone in rabbits as assessed by a bone chamber and intravital microscopy (Hsieh et al., 2001), we assumed that the present model is successful in inducing hypoxia in bones. As ischemia-reperfusion injury in bone has been hypothesized to lead to healing and remodelling processes (Zhang et al., 2017), we studied the effects of hypoxia-reoxygenation on bone over a period of up to seven days of reoxygenation to reveal any tissue adaptation that may occur at a later time point.

The present study showed that osteoblast precursors in the inner layer of the periosteum, osteoblasts, osteocytes and osteoclasts in control femurs were immunoreactive for HIF-1α and VEGF, the expression of which was upregulated following hypoxia-reoxygenation. This is consistent with a previous study reporting that HIF-1 protein is expressed in various tissues such as brain, kidney, liver, heart and skeletal muscle under normoxia and is further increased following exposure to systemic hypoxia (Stroka et al.,

2001).

Importantly, systemic hypoxia-reoxygenation was found to trigger apoptosis of cells from the osteogenic lineage in our animal model as well as cell death in our *in vitro* study using osteoblast-like SaOs-2 cells. This is in accordance with *in vitro* experiments by others showing that hypoxia promotes apoptosis of MC3TC-E1 osteoblast cells (Xu et al., 2015) and MLO Y4 osteocyte cells (Montesi et al., 2016) and may be relevant with respect to bone properties such as bone structure and strength (Jilka et al., 2013). The fact that we did not observe any evidence for hypoxia-triggered death of osteoclasts suggests that these cells may have a higher tolerance towards low oxygenation. This reasoning is supported by data from others indicating that hypoxia-reoxygenation enhances osteoclastogenesis (Arnett et al., 2003; Muzylak et al., 2006; Knowles and Athanasou, 2009; Utting et al., 2010). Along with the above mentioned changes, the present study showed endothelial cell death of the blood vessels within the bone marrow cavity following hypoxia. Similarly, others reported endothelial cell death in response to ischemia-reperfusion injury in heart tissue (Scarabelli et al., 2001).

Vital to the maintenance of normal cellular function under physiological and pathological conditions are molecular events that occur at subcellular levels such as in the ER. In postnatal rats in the present study, electron microscopy revealed pronounced dilatation of the ER in osteoblasts and osteocytes following systemic hypoxia-reoxygenation injury as opposed to control cells. Dilatation of ER cisternae displays a well-documented ultrastructural response to ER stress (Schönthal, 2012). The presence of ER stress following hypoxia-reoxygenation in the present study was supported by enhanced immunoexpression of the ER stress marker GRP78 (Lee, 2005) in osteoblasts and osteocytes in rat

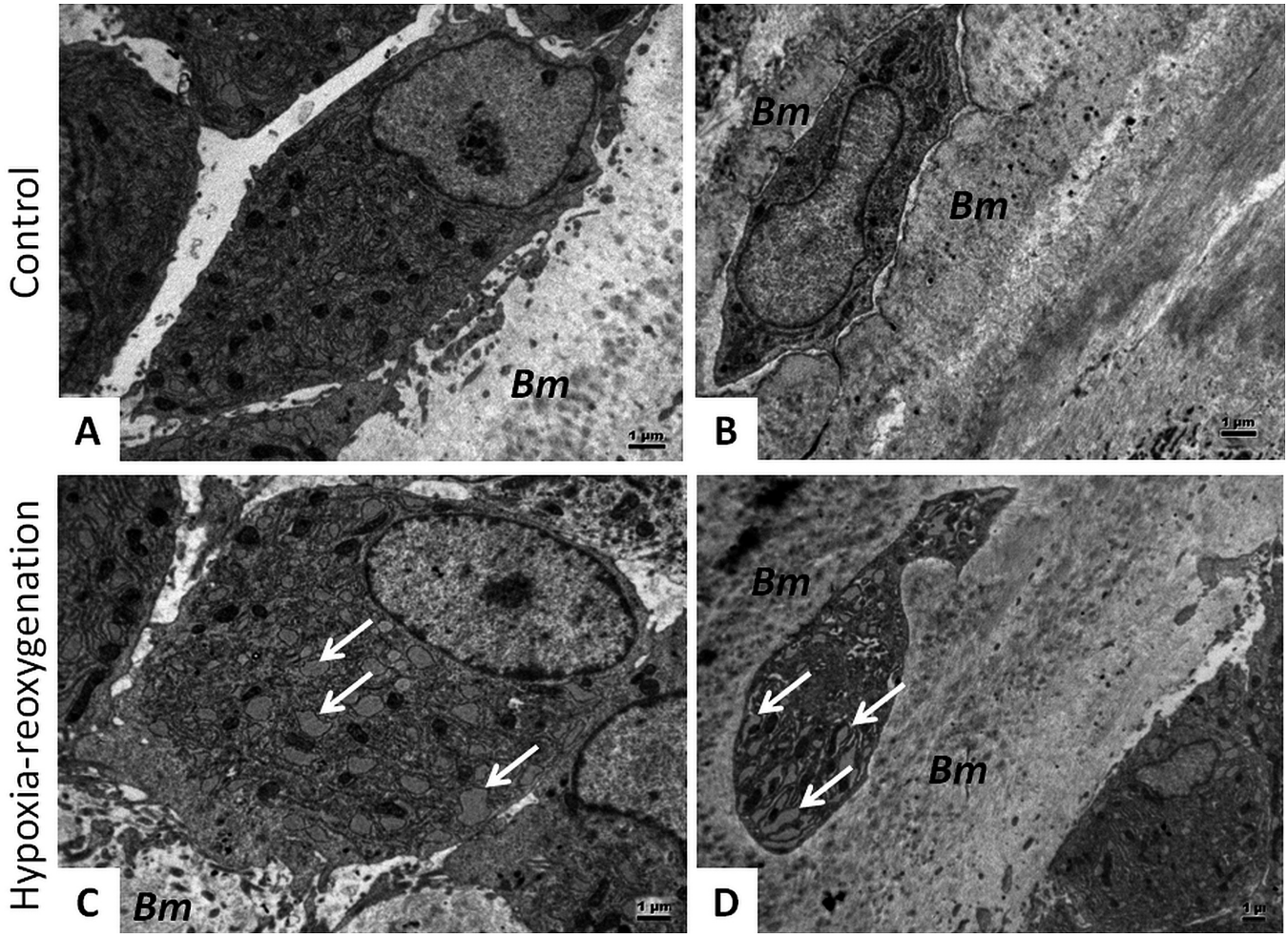

Fig. 7. Electron microscopic images displaying osteoblasts **(A, C)** and osteocytes **(B, D)** in femurs obtained from control Wistar rats **(A, B)** and at 3 days after hypoxia-reoxygenation injury **(C, D)**. Extensive dilatation of the endoplasmic reticulum (arrows) in osteblasts **(C)** and osteocytes **(D)** was observed after hypoxia-reoxygenation. Bm: bone matrix. Scale bars: A, B, 1 μm; C, 0.5 μm; D, 1 μm.

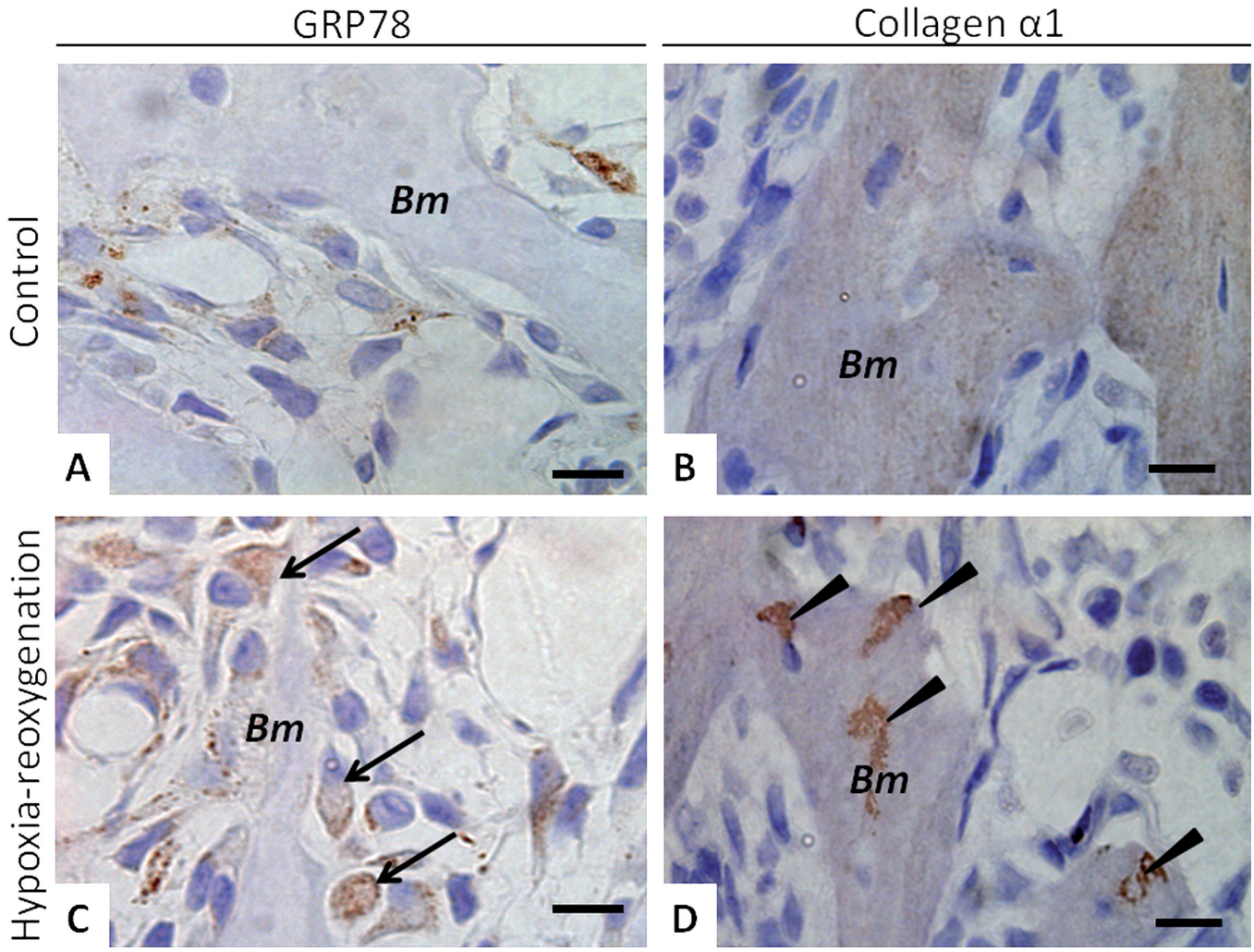

Fig. 8. Light microscopic images displaying osteoblasts and osteocytes in femurs obtained from control Wistar rats **(A, B)** and after hypoxia-reoxygenation injury **(C, D)**. Enhanced immunoexpression for the endoplasmic reticulum chaperone glucose-related protein78 (GRP78) was noted in osteoblasts (arrows) after hypoxia-reoxygenation **(C)** as compared to controls **(A)**. Immunoexpression for collagen α1 was widespread in the bone matrix of trabeculae in control femurs **(B)** but confined to osteocytes (arrowheads) in response to hypoxia-reoxygenation **(D)**. Bm: bone matrix. Scale bars: 10 μm.

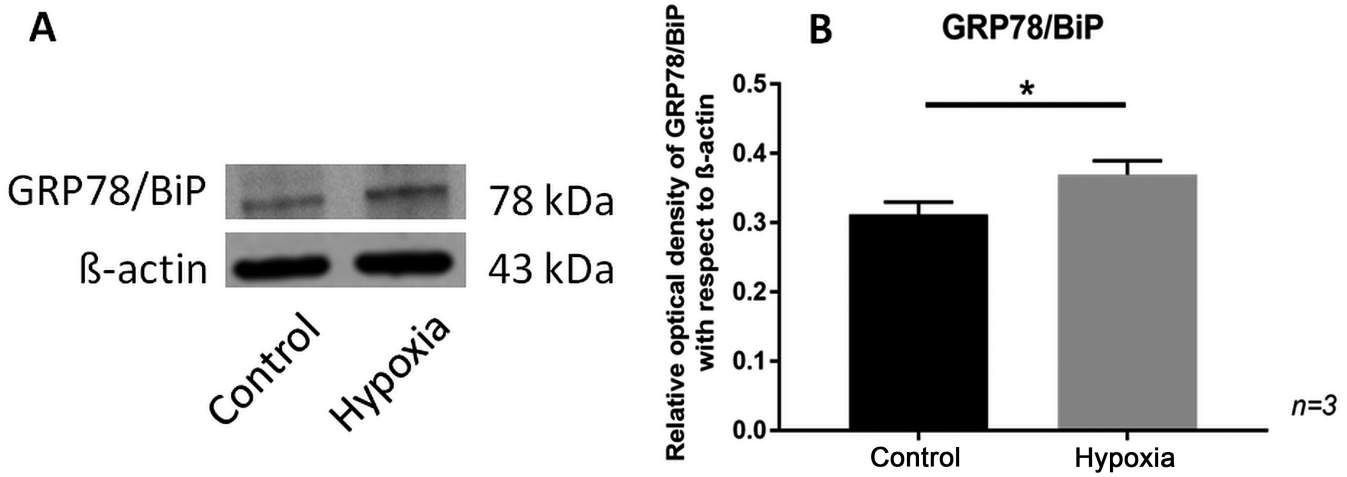

Fig. 9. Western blot of GRP78/BiP in normal and hypoxic osteoblast-like SAOS-2 cells. **A** shows the immunoreactive bands of GRP78/BiP (78 kDa) and ß-actin (43 kDa). **B** is the corresponding bar graph showing significant changes in GRP78/BiP protein expression following exposure to hypoxia (given as mean ± SD). The significant difference in GRP78/BiP protein level between hypoxic and control cells is expressed as *p<0.05.

femurs. Likewise, GRP78 protein expression was significantly upregulated in osteoblast-like SaOs-2 cells *in vitro* following exposure to hypoxia. This is in agreement with another study, which suggested that rheumatoid synoviocytes exhibit an increased GRP78 response to hypoxia (Yoo et al., 2012). Similarly, hypoxia increased GRP78 mRNA expression in endothelial cells (Yang et al., 2014). GRP78, also known as binding immunoglobulin protein (BiP), is an ER chaperone that gets activated when un- or misfolded proteins pile up and it is one of the initial elements that trigger the unfolded protein response (Quinones et al., 2008) in the attempt to restore the balance between protein load and folding capacity of the ER. Its regulatory role is further underlined by the ability to complex with pro-caspases (Lee, 2005). Thus, GRP78 coordinates cell survival and apoptosis in ER-stressed cells. The present study showed widespread positive immmunoreaction for collagen α1 in the bone matrix of control femurs as opposed to hypoxia-reoxygenation injury femurs, in which only osteoblasts and osteocytes displayed a strong immunoreaction for collagen α1. This observation promotes the idea that ER stress following hypoxia-reoxygenation may be based on the accumulation of collagen within osteoblasts and osteocytes.

Our study may be limited by differences in human and animal bone architecture as human bones are thought to comprise fewer but longer-living osteoblasts as compared to their murine counterparts (Jilka et al., 2013). In addition to that, biochemical differences in the composition of bones in the rat and human have been noted (Aerssens et al., 1998). To validate the findings derived from animal work, human osteoblast-like cells were chosen for the *in vitro* part of this study. We acknowledge, however, that immortalized cells may display different morphological, molecular and phenotypical characteristics as compared to native cells. The variability of statistical significance for the immunomarkers may be explained by differences in the temporal dynamics of protein expression in osteoblasts and osteocytes in response to hypoxia *in vivo*. To put things into perspective, the greatest effect of hypoxia on the immunomarkers in the animal model appeared to occur three days after the intervention. As we were not able to extract proteins of adequate quality from osteoblasts in animal tissue, a clear cause-effect relationship between ER-stress and apoptosis of osteoblasts and osteocytes following systemic hypoxia-reoxygenation remains to be determined. Future studies may like to examine the effect of systemic hypoxia-reoxygenation on osteoblast and osteoclast precursors, evaluating the osteoblastic and osteoclastic differentiation.

Conclusion

Using various light and electron microscopic techniques, our results suggest that systemic hypoxia-reoxygenation may disturb bone biology in postnatal Wistar rats by inducing ER stress and apoptosis in osteoblasts and osteocytes, without affecting the viability of osteoclasts. More research is needed to confirm causality between ER stress and apoptosis of osteoblasts and osteocytes.

Acknowledgements. This study was supported by research grant NMRC/CNIG/1147/2016 from National Medical Research Council of Singapore. The technical assistance provided by Mrs. Geok Lan Ng and Dr Wu Yajun is gratefully acknowledged.

There is no conflict of interest among the authors.

References

Aerssens J., Boonen S., Lowet G. and Dequeker J. (1998). Interspecies differences in bone composition, density and quality: potential implications for *in vivo* bone research. Endocrinology 139, 663-670.

Andersen C. (2001). Critical haemoglobin thresholds in premature infants. Arch. Dis. Child Fetal Neonatal Ed. 3, F146-468.

Austen W.G., Ebert P.A. and Greenfield L.J. (1963). Mechanisms of cardiac arrest in acute hypoxia. Surgery 53, 784-791.

Araldi E. and Schipani E. (2010). Hypoxia, HIFs and bone development. Bone 47, 190-196.

Arnett T.R., Gibbons D.C., Utting J.C., Orriss I.R., Hoebertz A., Rosendaal M. and Meghji S. (2003). Hypoxia is a major stimulator of osteoclast formation and bone resorption. J. Cell. Physiol. 196, 2-8.

Bradford M.M. (1976). A rapid and sensitive method for the quantification of microgram quantities of protein utilizing the principle of protein-dye binding. Anal. Biochem. 72, 248-254.

Hartung T. and Daston G. (2009). Are *in vitro* tests suitable for regulatory use? Toxicol. Sci. 2, 233-237.

Henriksen K., Karsdal M., Delaisse J.M. and Enqsiq M.T. (2003). RANKL and vascular endothelial growth factor (VEGF) induce osteoclast chemotaxis through an ERK1/2-dependent mechanism. J. Biol. Chem. 278, 48745-48753.

Hsieh A.S., Winet H., Bao J.Y., Glas H. and Plenk H. (2001). Evidence for reperfusion injury in cortical bone as a function of crush injury ischemia duration: A rabbit bone chamber study. Bone 28, 94-103.

Huang Y-C., Zhu H-M., Cai J-Q., Huang J-Z., Xu J., Zhou Y., Chen X-H., Li X-Q., Yang Z-M. and Deng L. (2012). Hypoxia inhibits the spontaneous calcification of bone marrow-derived mesenchymal stem cells. J. Cell Biochem. 113, 1407-1415.

Jilka R.L., Noble B. and Weinstein R.S. (2013). Osteocyte apoptosis. Bone 54, 264-271.

Kaur C., Sivakumar V., Foulds W.S., Luu C.D. and Ling E-A. (2009). Cellular and vascular changes in the retina of neonatal rats after an acute exposure to hypoxia. Invest. Ophthalmol. Vis. Sci. 50, 5364-5374.

Kaur C., Sivakumar V., Zou Z. and Ling E-A. (2014). Microglia-derived proinflammatory cytokines tumor necrosis factor-alpha and interleukin-1beta induce Purkinje neuronal apoptosis via their receptors in hypoxic neonatal rat brain. Brain Struct. Funct. 219, 151-170.

Kent B.D., Mitchell P.D. and McNickolas W.T. (2011). Hypoxemia in patients with COPD: cause, effects, and disease progression. Int. J. Cron. Obstruct. Pulmon. Dis. 6, 199-208.

Knowles H.J. and Athanasou N.A. (2009). Acute hypoxia and osteoclast

activity: A balance between enhanced resorption and increased apoptosis. J. Pathol. 218, 256-264.

Lee A.S. (2005). The ER chaperone and signaling regulator GRP78/BiP as a monitor of endoplasmic reticulum stress. Methods 35, 373-381.

Lennon D.P., Edmison J.M. and Caplan A.I. (2001). Cultivation of rat marrow-derived mesenchymal stem cells in reduced oxygen tension: Effects on *in vitro* and *in vivo* osteochondrogenesis. J. Cell Physiol. 187, 345-355.

Li J., Yang S., Li X., Liu D., Wang Z., Guo J., Tan N., Gao Z., Zhao X., Zhang J., Gou F., Yokota H. and Zhang P. (2017). Role of endoplasmic reticulum stress in disuse osteoporosis. Bone 97, 2-14.

Liu Y., Cox S.R., Morita T. and Kourembanas S. (1995). Hypoxia regulates vascular endothelial growth factor gene expression in endothelial cells. Identification of a 5' enhancer. Circulation Research. 77, 638-643.

Liu H., Zhu R., Liu C., Ma R., Wang L., Chen B., Li L., Niu J., Zhao D., Mo F., Fu M., Brömme D., Zhang D. and Gao S. (2017). Evaluation of decalcification techniques for rat femurs using HE and immunohistochemical staining. Biomed. Res. Int. 2017, 9050754.

Lisse T.S., Thiele F., Fuchs H., Hans W., Przemeck G.K.H., Abe K., Rathkolb B., Quintanilla-Martinez L., Hoelzlwimmer G., Helfrich M., Wolf E., Ralston S.H. and Hrabé de Angelis M. (2008). ER stress-mediated apoptosis in a new mouse model of osteogenesis imperfecta, PLoS Genet. 4, e7.

Maes C., Carmeliet E. and Schipani E. (2012). Hypoxia-driven pathways in bone development, regeneration and disease. Nat. Rev. Rheumatol. 8, 358-366.

Majmundar A.J., Wong W.J. and Simon M.C. (2011). Hypoxia inducible factors and the response to hypoxic stress. Mol. Cell 40, 294-309.

Miyauchi Y., Sato Y., Kobayashi T., Yoshida S., Mori T., Kanagawa H., Katsuyama E., Fujie A., Hao W., Miyamoto K., Tando T., Morioka H., Matsumoto M., Chambon P., Johnson R.S., Kato S., Toyama Y. and Miyamoto T. (2013). HIF1α is required for osteoclast activation by estrogen deficiency in postmenopausal osteoporosis, Proc. Natl. Acad. Sci. USA 110, 16568-16573.

Montesi M., Jähn K., Bonewald L., Stea S., Bordini B. and Beraudi A. (2016). Hypoxia mediates osteocyte ORP150 expression and cell death *in vitro*. Mol. Med. Rep. 14, 4248-4254.

Muzylak M., Price J.S. and Horton M.A. (2006). Hypoxia induces giant osteoclast formation and extensive bone resorption in the cat. Calcif. Tissue Int. 79, 301-309.

Nakagawa M., Kaneda T., Arakawa T., Morita S., Sato T., Yomada T., Hanada K., Kumegawa M. and Hakeda Y. (2000). Vascular endothelial growth factor (VEGF) directly enhances osteoclastic bone resorption and survival of mature osteoclasts. FEBS Lett. 473, 161-164.

Niida S., Kaku M., Amano H., Yoshida H., Katoka H., Nishikawa S., Tanne K., Maeda N., Nishikawa S. and Kodama H. (1999). Vascular endothelial growth factor can substitute for macrophage colony-stimulating factor in the support of osteoclastic bone resorption. J. Exp. Med. 190, 293-298.

Nizet V. and Johnson R.S. (2009). Interdependence of hypoxic and innate immune response. Nat. Rev. Immunol. 7165, 209-213.

Parfitt A.M. (1994). The spatial and temporal framework for signal traffic in adult human bone. J. Cell Biochem. 55, 273-286.

Pautke C., Schieker M., Tischer T., Kolk A., Neth P., Mutschler W. and Milz S. (2004). Characterization of osteosarcoma cell lines MG-63, Saos-2 and U-2 OS in comparison to human osetoblasts. Anticancer Res. 24, 3743-3748.

Potier E., Ferreira E., Andriamanalijaona R., Pujol J-P., Oudina K., Logeart-Avramoglou D. and Petite H. (2007). Hypoxia affects mesenchymal stromal cell osteogenic differentiation and angiogenic factor expression. Bone 40, 1078-1087.

Quinones Q.J., de Ridder G.G. and Pizzo S.V. (2008). GRP78: A chaperone with diverse roles beyond the endoplasmic reticulum. Histol. Histopathol. 23, 1409-1416.

RajendranNair D.S., Karunakaran J. and Nair R.R. (2017). Differential response of human cardiac stem cells and bone marrow mesenchymal stem cells to hypoxia-reoxygenation injury. Mol. Cell Biochem. 425, 139-153.

Rathnasamy G., Ling E-A. and Kaur C. (2011). Iron and iron regulatory proteins in amoeboid microglial cells are linked to oligodendrocyte death in hypoxic neonatal rat periventricular white matter through production of proinflammatory cytokines and reactive oxygen/nitrogen species. J. Neurosci. 31, 17982-17995.

Rathnasamy G., Sivakumar V., Foulds W.S., Ling E-A. and Kaur C. (2015). Vascular changes in the developing rat retina in response to hypoxia. Exp. Eye Res. 130, 73-86.

Reinders M.E., Sho M., Izawa A., Wang P., Mukhopadhay D., Koss K.E., Geehan C.S., Luster A.D., Savegh M.H. and Brioscoe D.M. (2003). Proinflammatory functions of vascular endothelial growth factor in alloimmunity. J. Clin. Invest. 112, 1655-1665.

Reynolds E.O. (1977). Hypoxia in the newborn infant. J. Clin. Pathol. Suppl. (R. Coll. Pathol). 11, 134-141.

Samelko L., Caicedo M.S., Lim S-J., Della-Valle C., Jacobs C. and Hallab N.J. (2013). Cobalt alloy implant debris induce HIF-1α hypoxia associated responses: A mechanism for metal-specific orthopedic implant failure. PloS One 8, e67127.

Scarabelli T., Stephanou A., Rayment N., Pasini E., Comini L., Curello S., Ferrari R., Knight R., and Latchman D. (2001). Apoptosis of endothelial cells precedes myocyte cell apoptosis in ischemia/reperfusion injury. Circulation 104, 253-256.

Schönenberger M.J. and Kovacs W.J. (2015). Hypoxia signaling pathways: modulators of oxygen-related organelles. Front. Cell Dev. 3, 42.

Schönthal A.H. (2012). Endoplasmic reticulum stress: Its role in disease and novel prospects for therapy. Scientifica (Cairo) 2012, 857516.

Seamon J., Keller T., Saleh J. and Cui Q. (2012). The pathogenesis of nontraumatic osteonecrosis. Arthritis 2012, 601763.

Stroka D.M., Burkhardt T., Desbaillets I., Wenger R.H., Neil D.A., Bauer C., Gassmann M. and Candinas D. (2001). HIF-1 is expressed in normoxic tissue and displays an organ-specific regulation under systemic hypoxia. FASEB J. 15, 2445-2453.

Tabas I. and Ron D. (2011). Integrating the mechanisms of apoptosis induced by endoplasmic reticulum stress. Nat. Cell Biol. 13, 184-190.

Utting J.C., Flanagan A.M., Brandao-Burch A., Orriss I.R. and Arnett T.R. (2010). Hypoxia stimulates osteoclast formation from human peripheral blood. Cell Biochem. Funct. 28, 374-380.

Xu G., Xue M., Wang H. and Xiang C. (2015). Hypoxia-inducible factor-1α antagonizes the hypoxia-mediated osteoblast cell viability reduction by inhibiting apoptosis. Exp. Ther. Med. 9, 1801-1806.

Yamada H., Nakajima T., Domon H., Honda T. and Yamazaki K. (2015). Endoplasmic reticulum stress response and bone loss in experimental periodontitis in mice. J. Periodontal Res. 50, 500-508.

Yang D., Gao L., Wang T., Qiao Z., Liang Y. and Zhang P. (2014). Hypoxia triggers endothelial endoplasmic reticulum stress and

apoptosis via induction of VLDL receptor. FEBS Lett. 588, 4448-4456.

Yoo S.A., You S., Yoon H.J., Kim D.H., Kim H.S., Lee K., Ahn J.H., Hwang D., Lee A.S., Kim K.J., Park Y.J., Cho C.S. and Kim W.U. (2012). A novel pathogenic role of the ER chaperone GRP78/BiP in rheumatoid arthritis. J. Exp. Med. 209, 871-886.

Zhang S., Wotzkow C., Bongoni A.K., Shaw-Boden J., Siegrist M., Taddeo A., Blank F., Hofstetter W. and Rieben R. (2017). Role of the plasma cascade systems in ischemia/reperfusion injury of bone. Bone 97, 278-286.

Accepted July 3, 2019